Journal of Alloys and Compounds 684 (2016) 29–33

Contents lists available at ScienceDirect

Journal of Alloys and Compounds

journal homepage: http://www.elsevier.com/locate/jalcom

Extraordinary magnetocaloric effect of Fe-based bulk glassy rods by combining fluxing treatment and J-quenching technique

Weiming Yang [a], Juntao Huo [b, **], Haishun Liu [a, *], Jiawei Li [b], Lijian Song [b], Qiang Li [c, ***], Lin Xue [d], Baolong Shen [d], Akihisa Inoue [b, e]

[a] School of Mechanics and Civil Engineering, State Key Laboratory for Geomechanics and Deep Underground Engineering, School of Sciences, China University of Mining and Technology, Xuzhou 221116, People's Republic of China
[b] Key Laboratory of Magnetic Materials and Devices, Ningbo Institute of Materials Technology & Engineering, Chinese Academy of Sciences, Ningbo 315201, People's Republic of China
[c] School of Physics Science and Technology, Xinjiang University, Urumqi, Xinjiang 830046, People's Republic of China
[d] School of Materials Science and Engineering, Southeast University, Nanjing 211189, People's Republic of China
[e] Department of Physics, King Abdulaziz University, Jeddah 21589, Saudi Arabia

ARTICLE INFO

Article history:
Received 23 March 2016
Received in revised form
12 May 2016
Accepted 14 May 2016
Available online 17 May 2016

Keywords:
Magnetocaloric effect
Fe-based glassy alloy
Fluxing treatment
J-quenching technique

ABSTRACT

The extraordinary magnetocaloric effect of $Fe_{80}P_{13}C_7$ bulk glassy rods has been studied. The magnetic entropy change (ΔS_M) and refrigerant capacity (*RC*) values under 1.5 T can reach 2.20 J kg^{-1} K^{-1} and 125 J kg^{-1}, respectively, which are the largest values among present ternary Fe-based glassy alloys. It is found that the magnetocaloric effect *vs* temperature curve gradually changes into two peaks with increasing magnetic fields, leading to a much wider ΔS_M peak and thus a larger *RC*. This extraordinary magnetocaloric effect in $Fe_{80}P_{13}C_7$ may be attributed to the coexistence of magnetic transition and spin reorientation transition.

1. Introduction

Magnetic refrigeration materials based on magnetocaloric effect (MCE), due to their great merits such as environmental friendliness and relatively high efficiency, have been regarded as a potential alternative energy source to replace the conventional gas compression/expansion refrigeration devices [1–6]. Until now, several intermetallic compounds such as Gd-Si-Ge [7], La-Ca-Mn-O [8], Ni-Mn-Ga [9], La-Fe-Si [10], Mn-Fe-P-As [11], Ni-Mn-Sn [12,13], etc., display giant MCE originating from their first order magneto-structural phase transitions. However, they are unfortunately accompanied by large thermal and magnetic hysteresis that reduces operation frequency in refrigerator appliances [14]. In contrast, soft magnetic materials are well known for their low hysteresis, owing to the fact that irreversible entropy can be avoided during magnetization and/or demagnetization [15]. Development of magnetic refrigerants based on soft magnetic materials could also allow the replacement of superconducting magnets with permanent magnets for producing an external magnetic field [16]. As excellent soft magnetic materials, Fe-based glassy alloys, unlike the crystalline materials in which the constituent atoms reside at thermodynamic equilibrium, are metastable materials in far-from-equilibrium states [17]. They have additional characteristics that are desirable for magnetic refrigerants: higher electrical resistivity than crystalline materials (which minimizes eddy current losses) [18,19], high corrosion resistance [20], tunable transition temperature by alloying [21], good mechanical properties (especially in the case of bulk metallic glasses) [22,23], negligible magnetic hysteresis, and low cost, etc. Moreover, these materials display negligible magnetic anisotropy fundamentally simplifies the study related to their magnetic transition, making them a good testing ground for analyzing the physics behind the MCE and for developing thermodynamic models to represent their response. An active magnetic regenerator system requires large MCE and plates-shaped or spherical particles with an optimal geometry to achieve the best

* Corresponding author.
** Corresponding author.
*** Corresponding author.
E-mail addresses: huojuntao@nimte.ac.cn (J. Huo), liuhaishun@126.com (H. Liu), qli@xju.edu.cn (Q. Li).

http://dx.doi.org/10.1016/j.jallcom.2016.05.142
0925-8388/

thermal transport properties between magnetic refrigerants and heat-exchange medium [24]. Therefore, the Fe-based glassy alloys with small MCE and low glass-forming ability (GFA) have hindered their development seriously for a long time. Fortunately, multi-element magnetocaloric Fe-based glassy alloys with larger GFA were synthesized by conventional copper mold casting very recently [25,26]. However, enhanced GFA inevitably leads to the deterioration of MCE; also, Fe-based glassy alloys with larger GFA generally contain large amount of expensive and easily oxidized metals (e.g. Zr, Nb, or rare earth), which limit their applications in magnetic refrigerants. It is a huge challenge to develop large MCE and GFA in Fe-based glassy alloys without any noble metals. A recent study shows that Fe-based glassy alloys without noble metals exhibiting excellent GFA can be synthesized by combining fluxing treatment and J-quenching technique [27]. It is interesting to explore the design of large MCE and GFA glassy alloy without noble metals with the help of this J-quenching technique.

Considering the large peak value of MCE Fe_2P-type compounds [11,28], we focused on the ternary $Fe_{80}P_{13}C_7$ alloy without any noble metals, which may consist of Fe_2P-type short range order clusters [29]. The goal of this study is to obtain $Fe_{80}P_{13}C_7$ alloy with large GFA by combining fluxing treatment and J-quenching technique, and to investigate its MCE systematically. The ternary magnetocaloric Fe-based bulk glassy alloy containing only one metallic element, which simplifies the related physics mechanism behind the MCE. This work is expected to enlighten further research on magnetocaloric effect of glassy alloys as promising magnetic refrigerants.

2. Experimental

Mother alloy ingots of $Fe_{80}P_{13}C_7$ (at. %) composition were prepared by torch-melting a mixture of pure Fe powders (99.9 mass %), graphite powders (99.95 mass %), and Fe_3P pieces (99.5 mass %) under a high-purity argon atmosphere. The alloy ingots were fluxed in a fluxing agent composed of B_2O_3 and CaO with a mass ratio of 3:1 at 1500 K for several hours under a vacuum of ~10 Pa. After fluxed treatment, the molten alloy was conducted in the drawn fused silica tubes, which consists of two different diameters connected to each other. The typical dimensions of larger tube are length 5–10 cm with inner/outer diameter being 11/13 mm. The smaller tubes have length, wall thickness and inner diameter as 5–10 cm, 0.1–0.2 mm and 1–2 mm, respectively. The tube was connected to a mechanical pump that evacuated to ~5×10^{-3} Torr. Subsequently, Ar gas with high purity (below 1 atm) was filled in the whole tube. The ingot was melted using a torch. To achieve rapid quenching, the melt was pushed into a smaller fuses tube. After this, the whole system was immediately transferred to a furnace that heated the melt to ~1450 K. 5 min later, the tube was removed from the furnace and quenched in cold water for several minutes. The $Fe_{80}P_{13}C_7$ liquid metal was cooled down to room temperature, and the cylindrical alloy samples with diameters of 1.0–2.0 mm and lengths of a few centimeters were prepared. The above method is called J-quenching technique [27]. To make comparison, $Fe_{80}P_{13}C_7$ and $(Fe_{0.76}B_{0.24})_{96}Nb_4$ glassy ribbons with a width of about 1 mm and thickness about 20–25 μm were both produced by single-roller melt spinning method. The nature of glassy samples was ascertained by D8 Advance X-ray diffraction (XRD) with Cu $K\alpha$ radiation and NETZSCH DSC-404 differential scanning calorimetry (DSC) with a heating rate of 0.67 K/s. The measurements of magnetic properties were carried out using a superconducting quantum interference device magnetometer (Quantum Design MPMS SQUID VSM). For the measurements, disk shapes of fully amorphous samples with thickness of ~0.5 mm cutting from $Fe_{80}P_{13}C_7$ bulk glassy rods with 1.00 mm were used. The temperature step was chosen as 3 K or 5 K in the vicinity of T_C, and 10 K for the regions far away from T_C. Considering the influence of demagnetizing fields on the magnetocaloric effect, the samples were placed with their cross-section perpendicular to the magnetic field direction. The sweeping rate of field is slow enough to ensure the data are recorded in an isothermal process.

3. Results and discussion

Fig. 1 shows the XRD and DSC data of $Fe_{80}P_{13}C_7$ glassy alloys in as-cast rods with diameter of 2.0 mm by J-quenching technique and as-quench ribbons by single-roller melt spinning method, respectively. From the XRD data, only broad peaks without crystalline peaks can be seen for all of these samples, verifying good glassy phase formation in as-cast and as-quench states. The thermal stability data of cast $Fe_{80}P_{13}C_7$ glassy rods and glassy ribbons were summarized in Table 1. The glass transition temperature T_g, crystallization temperature T_{x1}, T_{x2} and Curie temperature T_C of glassy ribbon are slightly less than that of the rod sample. It is mainly due to the different thermal conductivity of samples with different geometries and cooling rate. There is no obvious difference in exothermic peaks between the DSC results of rod- and ribbon-shaped alloys. The crystallization enthalpy ΔH_x for the glassy rod was similar to that of glassy ribbon within the experimental error. All these results are complementary to the XRD data shown in Fig. 1, indicating the fully amorphous structure of the cylinder sample.

In order to evaluate the MCE of this glassy alloy, isothermal magnetization map of M-H with increasing filed in temperature range of 500–650 K was displayed in Fig. 2(a). It can be seen that the magnetization saturates was achieved at low applied magnetic fields below the T_C as a result of a low number density of domain-wall pinning sites. On the other hand, the curves gradually change into straight lines with increasing temperatures near and above T_C, indicating the transitions from ferromagnetic to paramagnetic. Magnetic entropy change (ΔS_M) can be calculated from magnetization isotherms using the Maxwell relation [30]:

$$\Delta S_M = \mu_0 \int_0^{H_{max}} \left(\frac{\partial M}{\partial T}\right)_H dH \quad (1)$$

where μ_0 is the permeability of vacuum and H_{max} is the maximum applied field. The magnetic field with maximal value of 5 T was

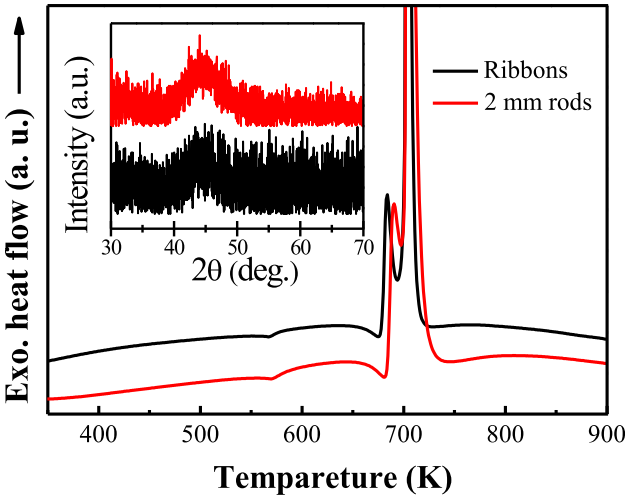

Fig. 1. XRD and DSC traces of as-cast $Fe_{80}P_{13}C_7$ glassy ribbons and rods.

Table 1
Thermal stability data of as-cast $Fe_{80}P_{13}C_7$ glassy rods with diameters up to 2.0 mm. The melt-spun glassy ribbons is also shown for comparison.

Samples	T_C (K)	T_g (K)	T_{x1} (K)	T_{x2} (K)	ΔH_x (J/g)
Ribbons	568	661	678	694	−90.05
Rods	570	665	683	699	−88.65

glassy rods was also presented in Fig. 3. Both $-\Delta S_M^{pk}$ and RC_{FWHM} tend to increase gradually with the magnetic field. For a better comparison, the $(Fe_{0.76}B_{0.24})_{96}Nb_4$ glassy ribbons with largest values of $-\Delta S_M^{pk}$ and RC_{FWHM} achieved in previous researches [25] were also shown in Fig. 3. Meanwhile, the reported ternary magnetocaloric Fe-based MGs and their GFA [14,32–38] including our

Table 2
Critical diameter and magnetocaloric properties under applied field of 1.5 T and 5 T for the present and reported typical ternary Fe-based glassy alloys.

Compositions (at.%)	Critical diameter	T_C (K)	$-\Delta S_M$ (J kg^{-1} K)		RC_{FWHM} (J kg^{-1})	References
			1.5 T	5 T	1.5 T	
$Fe_{80}P_{13}C_7$	Rods (2 mm)	579	2.20	5.05	125.6	This work
$(Fe_{0.76}B_{0.24})_{96}Nb_4$	Ribbons (D_C < 0.5 mm)	559	1.51	3.86	120.8	
$Fe_{88}Zr_8B_4$		285	–	3.30	–	[32]
$Fe_{91}Zr_7B_2$		230	–	2.80	–	
$Fe_{80}Cr_8B_{12}$		328	1.00	2.59	115	[33]
$Fe_{77}Cr_8B_{15}$		375	1.18	2.98	61	
$Fe_{84}Nb_7B_9$		299	1.44	–	–	[34]
$Fe_{79}Nb_7B_{14}$		372	1.07	–	–	
$Fe_{73}Nb_7B_{20}$		419	0.97	–	–	
$Fe_{86}Y_5Zr_9$		284	0.89	–	–	[35]
$Fe_{81}Y_{10}Zr_9$		470	1.12	–	–	
$Fe_{70}Mn_{10}B_{20}$		438	1.00	–	117	[36]
$Fe_{65}Mn_{15}B_{20}$		340	0.87	–	98	
$Fe_{60}Mn_{20}B_{20}$		210	0.60	–	83	
$Fe_{56}Mn_{24}B_{20}$		162	0.50	–	68	
$Fe_{85}Zr_{10}B_5$		300	1.39	–	–	[47]
$Fe_{82}Mn_8Zr_{10}$		210	–	2.78	–	[37]
$Fe_{84}Mn_6Zr_{10}$		218	–	2.29	–	
$Fe_{86}Mn_4Zr_{10}$		228	–	2.51	–	
$Fe_{80}Mn_{10}Zr_{10}$		195	–	2.33	–	
$Fe_{88}Sn_2Zr_{10}$		290	–	4.10	–	[38]
$Fe_{86}Sn_4Zr_{10}$		300	–	3.30	–	

used in our experiments. To derive the temperature dependence of ΔS_M, the numerical approximation of the integral is applied in this work, i.e.,

$$\Delta S_M(T_i, H) = \frac{\int_0^H M(T_i, H)dH - \int_0^H M(T_{i+1}, H)dH}{T_i - T_{i+1}} \quad (2)$$

By the isothermal *M-H* curves at various temperatures, we evaluate the ΔS_M associated with *H* variations according to Eq. (2). Fig. 2(b) shows the $-\Delta S_M$ of $Fe_{80}P_{13}C_7$ glassy rods as a function of temperature under 1.5–5 T. As shown in Fig. 2(b), the peak and width of $-\Delta S_M$ are dependent on the change of *H*, both the height and width increase obviously with the increasing filed. The peak values of $-\Delta S_M$ are 2.20 J kg^{-1} K^{-1} under 1.5 T, and 5.05 J kg^{-1} K^{-1} under 5 T, respectively. It is worth noticing that the increasing of *H* yields two separated magnetic entropy peaks. The separation between these two peaks is practically insensitive to the further increase of *H* beyond a small, critical value ~2 T. Another relevant parameter characterizing the refrigerant efficiency of the material is the refrigerant capacity (*RC*). We estimated *RC* by the product of the peak entropy change and the full width at half maximum of the peak as follows [31].

$$RC_{FWHM} = -\Delta S_M^{pk} \times \delta T_{FWHM} \quad (3)$$

where δT_{FWHM} was defined as the temperature interval of the full width at half maximum of $-\Delta S_M$. The separation of $-\Delta S_M$ peaks further increase δT_{FWHM}. We can see that the *RC* values of $Fe_{80}P_{13}C_7$ bulk glassy rods are about 125 J kg^{-1} under 1.5 T, and 480 J kg^{-1} under 5 T, respectively.

The field dependence of $-\Delta S_M^{pk}$ and RC_{FWHM} for $Fe_{80}P_{13}C_7$ bulk materials (for studies will be publish through May 2016) were listed in Table 2. Up to the time of writing, the largest $-\Delta S_M^{pk}$ and RC_{FWHM} achieved for $Fe_{80}P_{13}C_7$ bulk glassy rods by combining fluxing treatment and J-quenching technique were 2.20 J kg^{-1} K^{-1} and 125 J kg^{-1} under 1.5 T, respectively. These values place the present series of ternary Fe-based bulk glassy alloys among the best magnetic refrigerant materials, with $-\Delta S_M^{pk}$ ~46% larger than $(Fe_{0.76}B_{0.24})_{96}Nb_4$ glassy ribbons and *RC* ~35% larger than $Gd_5Si_2Ge_{1.9}Fe_{0.1}$ (355 J kg^{-1} under 5 T) [39]. It is worth mentioning that the largest magnetocaloric response in $Fe_{80}P_{13}C_7$ bulk glassy rods was achieved with lager GFA without any noble metals (e.g. Zr, Nb, or rare earth). As expected, enhancing GFA for $Fe_{80}P_{13}C_7$ alloy with no deleterious influence on $-\Delta S_M^{pk}$ and RC_{FWHM} was achieved, i.e. a balance between these two parameters could be obtained. According to the mean field theory [40], $|\Delta S_M^{pk}|$ and *RC* can be expressed approximately as $|\Delta S_M^{pk}| \propto AH^n$ and $RC \propto BH^p$, respectively. The exponents *n* and *p*, controlled by the critical exponents of these alloys, can be extracted through fitting the experimental data in Fig. 3(a) and (b) with the relations discussed above. The exponents $n = 0.69$ near the transition temperature for $Fe_{80}P_{13}C_7$ glassy rods are smaller than those for $(Fe_{0.76}B_{0.24})_{96}Nb_4$ (~0.77) and other Fe-based MGs (~0.75) [41], which consists with the predicted value (2/3) by the mean field theory [40]. It means that the fluctuations and heterogeneities in magnetic microstructures of $Fe_{80}P_{13}C_7$ glassy materials can be neglected [42].

According to the Maxwell relations, the larger MCE is due to the larger magnetic moment and the values of dM/dT near the Curie temperature in materials. Fig. 4 shows the temperature dependence of magnetization for $Fe_{80}P_{13}C_7$ and $(Fe_{0.76}B_{0.24})_{96}Nb_4$ glassy samples. It is well know that the saturation magnetization of $Fe_{80}P_{13}C_7$ is larger than that of $(Fe_{0.76}B_{0.24})_{96}Nb_4$. Even though the strong disorder effect exists in $Fe_{80}P_{13}C_7$ samples, the

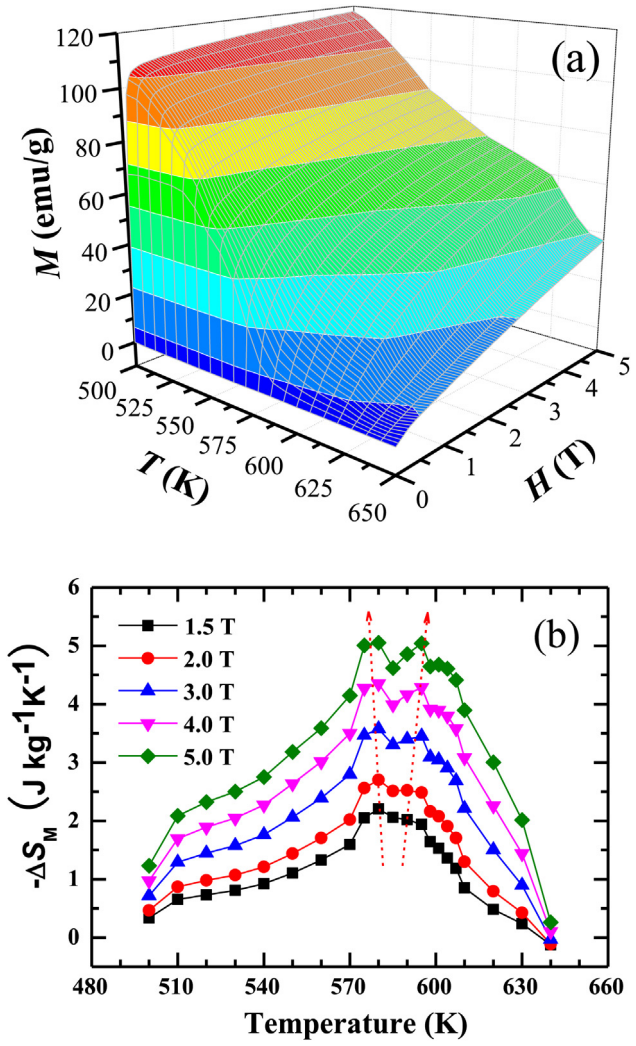

Fig. 2. (a) 3-dimensional magnetic entropy changes as a function of the temperature and applied magnetic field for $Fe_{80}P_{13}C_7$ glassy rods. (b) Magnetic entropy changes as a function of temperature under 1.5–5 T for $Fe_{80}P_{13}C_7$ bulk glassy rods.

magnetization varies sharply at the ordering temperature as that in the known crystalline magnetic refrigerant material of MnFeP$_{0.45}$As$_{0.55}$ [11]. The dM/dT vs. T of $Fe_{80}P_{13}C_7$ and of $(Fe_{0.76}B_{0.24})_{96}Nb_4$ glassy samples were plotted and shown in Fig. 5. We can see that the value of dM/dT for $Fe_{80}P_{13}C_7$ is also larger than that of $(Fe_{0.76}B_{0.24})_{96}Nb_4$. The origin of the rapidly changing magnetization is the magnetic quantum (magnetic spin waves) with exchange interaction and temperature-induced homogeneous magnetic phase abrupt transition near T_C [43,44]. From above analysis, we conclude that the origin of the large magnetic entropy change is in the comparatively high 3d moments and in the rapid change of magnetization. In this process, the strong magneto-crystalline coupling results in competing intra- and inter-atomic interactions, leading to a modification of Fe-Fe distances which may favor the spin ordering [45]. The two peaks of $-\Delta S_M$ may be caused by coexistence of the magnetic transition and spin reorientation transition when the applied magnetic field H is larger than the spin reorientation field of Fe-P-C system [46].

4. Conclusion

In summary, the extraordinary magnetocaloric effect in $Fe_{80}P_{13}C_7$ bulk glassy rods without noble metals prepared by

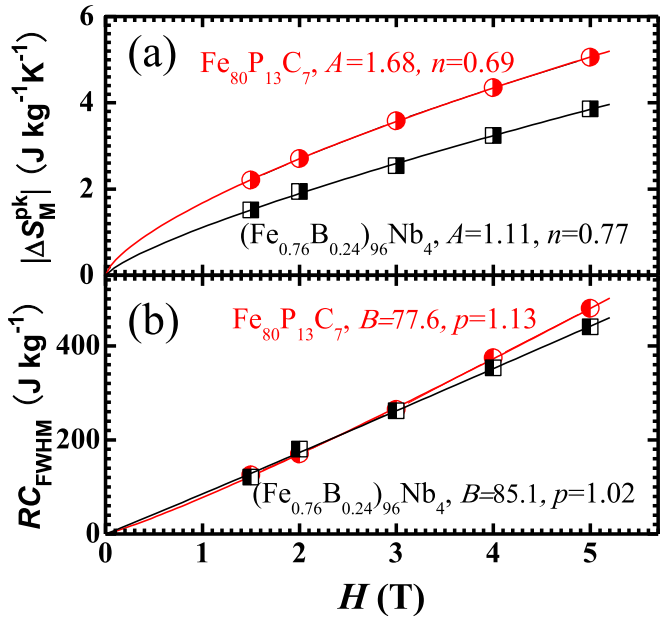

Fig. 3. Magnetic field dependence of the (a) maximum magnetic entropy changes $|\Delta S_M^{pk}|$, and (b) RC for $Fe_{80}P_{13}C_7$ and $(Fe_{0.76}B_{0.24})_{96}Nb_4$ glassy samples. The solid curves are fitting results of $|\Delta S_M^{pk}| \propto AH^n$ and $RC \propto BH^p$, respectively.

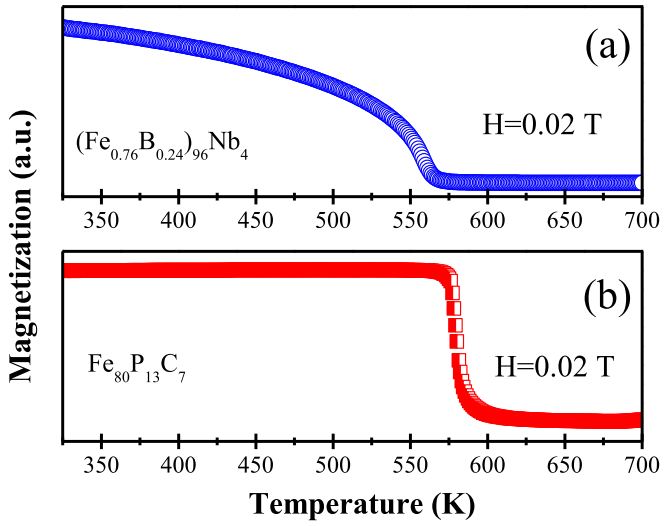

Fig. 4. (a) Temperature dependence of the magnetization for $(Fe_{0.76}B_{0.24})_{96}Nb_4$ glassy samples. (b) Temperature dependence of the magnetization for $Fe_{80}P_{13}C_7$ glassy samples.

combining fluxing treatment and J-quenching technique was investigated. The $-\Delta S_M^{pk}$ are 2.20 J kg^{-1} K^{-1} under 1.5 T, and 5.05 J kg^{-1} K^{-1} under 5 T, respectively. The RC are about 125 J kg^{-1} under 1.5 T, and 480 J kg^{-1} under 5 T, respectively. These values place the present ternary Fe-based bulk glassy alloys among the best magnetic refrigerant materials, with $-\Delta S_M^{pk}$ ~46% larger than $(Fe_{0.76}B_{0.24})_{96}Nb_4$ glassy ribbons and RC ~35% larger than crystalline $Gd_5Si_2Ge_{1.9}Fe_{0.1}$. The temperature dependence of magnetization in this alloy was also found. The origin of this extraordinary magnetic behavior was discussed. This work will enlighten further research on magnetocaloric effect of glassy alloys as promising magnetic refrigerants and supply a good opportunity for further analyzing the physics behind the MCE and for developing thermodynamic models to represent their response.

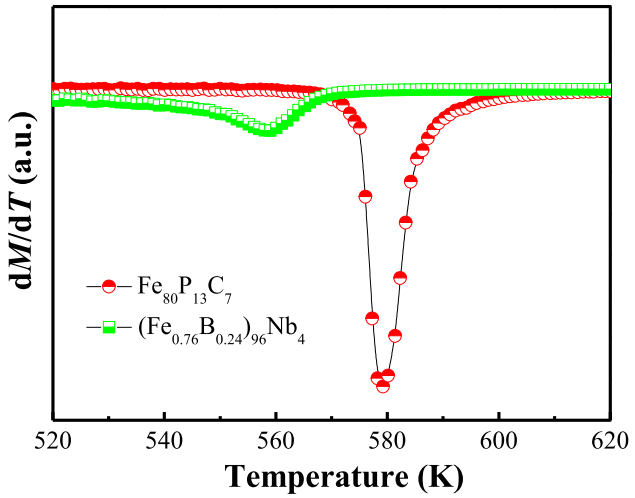

Fig. 5. The dM/dT under a magnetic field of 0.02T for $Fe_{80}P_{13}C_7$ and $(Fe_{0.76}B_{0.24})_{96}Nb_4$ glassy samples.

Acknowledgements

Weiming Yang is very grateful for financial support of the Fundamental Research Funds for the Central Universities (No. 2015XKZD02), the National Natural Science Foundation of China (No. 51501220), Qiang Li thank the National Natural Science Foundation of China (No. 51261028 and 51561028), and Jiawei Li thank the National Natural Science Foundation of China (No. 51501210).

References

[1] V. Franco, J. Blázquez, B. Ingale, A. Conde, The magnetocaloric effect and magnetic refrigeration near room temperature: materials and models, Mater. Res. 42 (2012) 305.
[2] O. Gutfleisch, M.A. Willard, E. Brück, C.H. Chen, S. Sankar, J.P. Liu, Magnetic materials and devices for the 21st century: stronger, lighter, and more energy efficient, Adv. Mater. 23 (2011) 821–842.
[3] Q. Luo, B. Schwarz, N. Mattern, J. Shen, J. Eckert, Roles of hydrogenation, annealing and field in the structure and magnetic entropy change of Tb-based bulk metallic glasses, AIP Adv. 3 (2013) 032134.
[4] P. Yu, N.Z. Zhang, Y.T. Cui, L. Wen, Z.Y. Zeng, L. Xia, Achieving an enhanced magneto-caloric effect by melt spinning a $Gd_{55}Co_{25}Al_{20}$ bulk metallic glass into amorphous ribbons, J. Alloys Compd. 655 (2016) 353–356.
[5] H. Shen, H. Wang, J. Liu, D. Xing, F. Qin, F. Cao, D. Chen, Y. Liu, J. Sun, Enhanced magnetocaloric and mechanical properties of melt-extracted $Gd_{55}Al_{25}Co_{20}$ micro-fibers, J. Alloys Compd. 603 (2014) 167–171.
[6] Q. Luo, W.H. Wang, Magnetocaloric effect in rare earth-based bulk metallic glasses, J. Alloys Compd. 495 (2010) 209–216.
[7] C. Wu, Y. Huang, J. Shen, Microscopic structural evolution during elastic deformation of $Fe_{65}Mo_{14}C_{15}B_6$ amorphous alloy studied by ab initio molecular dynamics simulations, Comput. Mater. Sci. 56 (2012) 6–10.
[8] H. Tian, C. Zhang, J. Zhao, C. Dong, B. Wen, Q. Wang, First-principle study of the structural, electronic, and magnetic properties of amorphous Fe–B alloys, Phys. B 407 (2012) 250–257.
[9] F.-X. Hu, B.-G. Shen, J.-R. Sun, Magnetic entropy change in $Ni_{51.5}Mn_{22.7}Ga_{25.8}$ alloy, Appl. Phys. Lett. 76 (2000) 3460.
[10] F.-X. Hu, B.-G. Shen, J.-R. Sun, Z.H. Cheng, G.H. Rao, X.-X. Zhang, Influence of negative lattice expansion and metamagnetic transition on magnetic entropy change in the compound $LaFe_{11.4}Si_{1.6}$, Appl. Phys. Lett. 78 (2001) 3675–3677.
[11] O. Tegus, E. Brück, K. Buschow, F. De Boer, Transition-metal-based magnetic refrigerants for room-temperature applications, Nature 415 (2002) 150–152.
[12] Y. Zhang, Q. Zheng, W. Xia, J. Zhang, J. Du, A. Yan, Enhanced large magnetic entropy change and adiabatic temperature change of $Ni_{43}Mn_{46}Sn_{11}$ alloys by a rapid solidification method, Scr. Mater. 104 (2015) 41–44.
[13] H.S. Liu, C.L. Zhang, Z.D. Han, H.C. Xuan, D.H. Wang, Y.W. Du, The effect of Co doping on the magnetic entropy changes in $Ni_{44-x}Co_xMn_{45}Sn_{11}$ alloys, J. Alloys Compd. 467 (2009) 27–30.
[14] Y. Wang, X. Bi, The role of Zr and B in room temperature magnetic entropy change of FeZrB amorphous alloys, Appl. Phys. Lett. 95 (2009) 262501–262503.
[15] J.W. Li, D. Estévez, K.M. Jiang, W.M. Yang, Q.K. Man, C.T. Chang, X.M. Wang, Electronic-structure origin of the glass-forming ability and magnetic properties in Fe–RE–B–Nb bulk metallic glasses, J. Alloys Compd. 617 (2014) 332–336.
[16] V. Pecharsky, K. Gschneidner Jr., Magnetocaloric effect from indirect measurements: magnetization and heat capacity, J. Appl. Phys. 86 (1999) 565–575.
[17] J.Q. Wang, Y.H. Liu, M.W. Chen, G.Q. Xie, D.V. Louzguine-Luzgin, A. Inoue, J.H. Perepezko, Rapid degradation of azo dye by Fe-based metallic glass powder, Adv. Funct. Mater. 22 (2012) 2567–2570.
[18] R. Caballero-Flores, V. Franco, A. Conde, K. Knipling, M. Willard, Influence of Co and Ni addition on the magnetocaloric effect in $Fe_{88-2x}Co_xNi_xZr_7B_4Cu_1$ soft magnetic amorphous alloys, Appl. Phys. Lett. 96 (2010), 182506–182503.
[19] S. Meng, H. Ling, Q. Li, J. Zhang, Development of Fe-based bulk metallic glasses with high saturation magnetization, Scr. Mater. 81 (2014) 24–27.
[20] S.J. Pang, T. Zhang, K. Asami, A. Inoue, Synthesis of Fe-Cr-Mo-C-B-P bulk metallic glasses with high corrosion resistance, Acta Mater. 50 (2002) 489–497.
[21] W.M. Yang, H.S. Liu, L. Xue, J.W. Li, C.C. Dun, J.H. Zhang, Y.C. Zhao, B.L. Shen, Magnetic properties of $(Fe_{1-x}Ni_x)_{72}B_{20}Si_4Nb_4$ (x=0.0–0.5) bulk metallic glasses, J. Magn. Magn. Mater. 335 (2013) 172–176.
[22] W. Yang, H. Liu, Y. Zhao, A. Inoue, K. Jiang, J. Huo, H. Ling, Q. Li, B. Shen, Mechanical properties and structural features of novel Fe-based bulk metallic glasses with unprecedented plasticity, Sci. Rep. 4 (2014) 6233.
[23] W. Yang, B. Sun, Y. Zhao, Q. Li, L. Hou, N. Luo, C. Dun, C. Zhao, Z. Ma, H. Liu, B. Shen, Non-repeatability of large plasticity for Fe-based bulk metallic glasses, J. Alloys Compd. 676 (2016) 209–214.
[24] A. Smith, C.R. Bahl, R. Bjørk, K. Engelbrecht, K.K. Nielsen, N. Pryds, Materials challenges for high performance magnetocaloric refrigeration devices, Adv. Energy Mater. 2 (2012) 1288–1318.
[25] J. Li, J. Huo, J. Law, C. Chang, J. Du, Q. Man, X. Wang, R.-W. Li, Magnetocaloric effect in heavy rare-earth elements doped Fe-based bulk metallic glasses with tunable Curie temperature, J. Appl. Phys. 116 (2014) 063902.
[26] M. Zhang, J. Li, F. Kong, J. Liu, Magnetic properties and magnetocaloric effect of FeCrNbYB metallic glasses with high glass-forming ability, Intermetallics 59 (2015) 18–22.
[27] Q. Li, Formation of ferromagnetic bulk amorphous $Fe_{40}Ni_{40}P_{14}B_6$ alloys, Mater. Lett. 60 (2006) 3113–3117.
[28] Y. Ma, D. Dong, C. Dong, L. Luo, Q. Wang, J. Qiang, Y. Wang, Composition formulas of binary eutectics, Sci. Rep. 5 (2015) 17880.
[29] P.K. Rastogi, Crystallization behaviour of an amorphous FePC alloy, J. Mater. Sci. 8 (1973) 140–143.
[30] T. Hashimoto, T. Numasawa, M. Shino, T. Okada, Magnetic refrigeration in the temperature range from 10 K to room temperature: the ferromagnetic refrigerants, Cryogenics 21 (1981) 647–653.
[31] K. Gschneidner Jr., V. Pecharsky, Magnetocaloric materials, Annu. Rev. Mater. Sci. 30 (2000) 387–429.
[32] Y. Geng, Y. Wang, J. Qiang, G. Zhang, C. Dong, P. Häussler, Composition formulas of Fe–B binary amorphous alloys, J. Non-Cryst. Solids 432 (2016) 453–458.
[33] G.-P. Zheng, A density functional theory study on the deformation behaviors of Fe-Si-B metallic glasses, Int, J. Mol. Sci. 13 (2012) 10401–10409.
[34] X. Gu, S.J. Poon, G.J. Shiflet, M. Widom, Mechanical properties, glass transition temperature, and bond enthalpy trends of high metalloid Fe-based bulk metallic glasses, Appl. Phys. Lett. 92 (2008), 161910–161910.
[35] P. Ganesh, M. Widom, Ab initio simulations of geometrical frustration in supercooled liquid Fe and Fe-based metallic glass, Phys. Rev. B 77 (2008) 014205.
[36] M. Aykol, A. Mekhrabov, M. Akdeniz, Nano-scale phase separation in amorphous Fe–B alloys: atomic and cluster ordering, Acta Mater. 57 (2009) 171–181.
[37] M. Marqués, L. González, D. González, Ab initio study of the structure and dynamics of bulk liquid Fe, Phys. Rev. B 92 (2015) 134203.
[38] T.L. Phan, N.H. Dan, T.D. Thanh, N.T. Mai, T.A. Ho, S.C. Yu, A.-T. Le, M.H. Phan, Magnetic properties and magnetocaloric effect in $Fe_{90-x}Sn_xZr_{10}$ alloy ribbons, J. Kor. Phys. Soc. 66 (2015) 1247–1252.
[39] V. Provenzano, A.J. Shapiro, R.D. Shull, Reduction of hysteresis losses in the magnetic refrigerant $Gd_5Ge_2Si_2$ by the addition of iron, Nature 429 (2004) 853–857.
[40] H. Oesterreicher, F. Parker, Magnetic cooling near Curie temperatures above 300 K, J. Appl. Phys. 55 (1984) 4334–4338.
[41] H. Zhang, R. Li, T. Xu, F. Liu, T. Zhang, Near room-temperature magnetocaloric effect in FeMnPBC metallic glasses with tunable Curie temperature, J. Magn. Magn. Mater. 347 (2013) 131–135.
[42] J. Huo, L. Huo, J. Li, H. Men, X. Wang, A. Inoue, C. Chang, J.-Q. Wang, R.-W. Li, High-entropy bulk metallic glasses as promising magnetic refrigerants, J. Appl. Phys. 117 (2015) 073902.
[43] C. Tsuei, G. Longworth, S. Lin, Temperature dependence of the magnetization of an amorphous ferromagnet, Phys. Rev. 170 (1968) 603.
[44] C.C. Tsuei, H. Lilienthal, Magnetization distribution in an amorphous ferromagnet, Phys.Rev. B 13 (1976) 4899–4906.
[45] W. Yang, The origin of rapid change of magnetization in Fe-P-C glassy systems, 2016. Unpublished.
[46] M. Shao, S. Cao, Y. Wang, S. Yuan, B. Kang, J. Zhang, Large magnetocaloric effect in $HoFeO_3$ single crystal, Solid State Commun. 152 (2012) 947–950.
[47] C. Hostert, D. Music, J. Bednarcik, J. Keckes, V. Kapaklis, B. Hjörvarsson, J. Schneider, Ab initio molecular dynamics model for density, elastic properties and short range order of Co–Fe–Ta–B metallic glass thin films, J. Phys. Condens. Matter 23 (2011) 475401.